Electronic Supplementary Information (ESI) for:

HCl chemisorption induced drastic magneto-structural transformation in a layered cobalt-phosphonotriazolate coordination Polymer

Weiquan Zhang,[†,¶] *Dianpeng Wang,*[‡,¶] *Lin Zhu,*[§,*] *Fupeng Zhai,*[†] *Linhong Weng,*[†,*] *Jinyu Sun,*[‡] *Yun Ling,*[†] *Zhenxia Chen,*[†,*] and *Yaming Zhou*[†]

[†] Shanghai Key Laboratory of Molecular Catalysis and Innovative Materials, Department of Chemistry, Fudan University, Shanghai, 200433, China.

[‡] Department of Chemistry, Liaoning University, Shenyang, 110036, China.

[§] School of Physics, Huazhong University of Science and Technology, Wuhan 430074, China

[¶] These two authors contribution equally to this work

[*] Corresponding authors: zhxchen@fudan.edu.cn (Prof. Chen, Z.X.);

linzh@hust.edu.cn (Prof. Zhu L.);

lhweng@fudan.edu.cn (Prof. Weng L.H.)

1. Materials and General Methods.

All reagents were purchased from commercial sources and used without further purification. 4-(1,2,4-triazol-4-yl)phenylphosphonic acid (H_2ptz) was prepared by the procedure reported in our previous literature.[1] IR spectra (KBr pellets) were recorded on a Nicolet 470 FT-IR spectrometer in the range 4000 - 400 cm^{-1}. C, H and N elemental analyses were determined on the Elementar Vario EL III. The crystal phase was confirmed by powder X-ray diffraction collected on a Bruker D8 powder diffractometer with Cu-Kα radiation (λ = 1.5406 Å). Thermal stability studies were carried out on a TGA/SDTA 851 thermoanalyzer in the temperature range of 35-800 °C under N_2 flow at a heating rate of 10 $°C \cdot min^{-1}$. Magnetic measurement was carried out on a MPMS (SQUID) VSM magnetometer equipped with a 7 T magnet. Samples were restrained in eicosane to prevent torquing. The variable-temperature (2-300K) magnetic susceptibility was measured with an external magnetic field of 1000 Oe. Pascal's constants were used to estimate the diamagnetic corrections, which were subtracted from the experimental susceptibilities to give the molar paramagnetic susceptibilities (χ_m). The magnetization isotherm was collected at 2 K between -7 and 7 T.

Theoretical calculation is based on the density functional theory (DFT) with generalized gradient approximation (PBE-GGA), using the accurate full-potential linearized augmented plane wave (FPLAPW), WIEN2K code has been used to execute the calculation. The crystal structures of **Coptz-1** and **Coptz-2** are directly used.

[1]. F. Zhai, Q. Zheng, Z. Chen, Y. Ling, X. Liu, L. Weng and Y. Zhou, CrystEngComm, 2013, 15, 2040-2043.

2. Synthesis

[Co(ptz)·H_2O]$_n$ (Coptz-1): A mixture of $Co(NO_3)_2\cdot 6H_2O$ (0.088 g, 0.30 mmol), H_2ptz (0.068 g, 0.30 mmol), triethylamine (0.101 g, 1.0 mmol) and deionized water (10 mL) was placed in a teflon-lined stainless steel autoclave (15 mL) and was stirred at room temperature for 1 h. The mixture was then heated at 180 °C for 24 h, followed by cooling down to room temperature. Dark-red sheet crystals were collected by filtration. Yield: 67% (0.060 g, based on H_2ptz). Elemental analysis calcd. for $C_8H_8N_3CoO_4P$ (300.07): C, 32.02; H, 2.69; N, 14.00 %. Found: C, 31.96; H, 2.77; N, 14.12 %. IR (KBr, cm^{-1}) 3371 (b), 3155 (w), 3094 (w), 1530 (s), 1411 (m), 1322 (w), 1253 (m), 1123 (m), 1057 (m), 991(m), 970 (m), 830 (w), 743 (w), 626 (w), 587 (m), 450 (w).

[Cu(ptz) ·H_2O]$_n$ (Cuptz-1): A mixture of $Cu(Ac)_2\cdot H_2O$ (0.030g, 0.15 mmol), H_2ptz (0.068 g, 0.30 mmol), LiAc·$2H_2O$ (0.031g, 0.45 mmol) and deionized water (10 mL) was placed in a teflon-lined stainless steel autoclave (15 mL) and was stirred at room temperature for 1 h. The mixture was then heated at 140 °C for 48 h, followed by cooling down to room temperature. Light-green sheet crystals were collected by filtration. Yield 92% (0.042 g, based on $Cu(Ac)_2\cdot H_2O$). Elemental analysis calcd. for $C_8H_8N_3CuO_4P$ (304.68): C, 31.53; H, 2.65; N, 13.79 %, Found C, 31.42; H, 2.71; N, 13.92 %. IR (KBr, cm^{-1}) 3425 (b), 3164 (w), 3052 (w), 1553 (s), 1414 (m), 1323 (w), 1256 (m), 1125 (m), 1049 (m), 994(m), 973 (m), 831 (w), 747 (w), 624 (w), 585 (m), 453 (w).

[Fe(ptz)·H_2O]$_n$ (Fepzt-1): A mixture of $FeSO_4\cdot 7H_2O$ (0.084 g, 0.30 mmol), H_2ptz (0.068 g, 0.30 mmol), triethylamine (0.050 g, 0.50 mmol) and deionized water (10 mL) was placed in a teflon-lined stainless steel autoclave (15 mL) and was stirred at room temperature for 1 h. The mixture was then heated at 180 °C for 24 h, followed by cooling down to room temperature. Light-green sheet crystals were collected by filtration. Yield 36% (0.032 g, based on H_2ptz). Elemental analysis calcd. for $C_8H_8N_3FeO_4P$ (296.99): C, 32.35; H, 2.72; N, 14.15 %. Found: C, 31.32; H, 2.77; N, 14.22 %. IR (KBr, cm^{-1}) 3268 (b), 3151 (w), 3095 (w), 1542 (s), 1412 (m), 1322 (w), 1253 (m), 1125 (m), 1045 (m), 992(m), 970 (m), 828 (w), 746 (w), 625 (w), 587 (m), 446 (w).

3. Phase transformation

Aqueous HCl (37%) 5 mL was added into a glass tube (A, 50 mL) with a glass stopper. 30 mg (0.1 mmol) of crystalline **Coptz-1** solid was added into a 10 mL glass tube, and then put it into the 50 mL glass tube and sealed. The phase transformation from **Coptz-1** to **Coptz-2** could be occurred in 20 minutes at 30 °C, in which process its color was changed from dark red to light blue after 8 mins, and then deep blue after 15 mins, then it transfers into gray-pink after the completion of phase transformation. Elemental analysis calcd. for $C_8H_{11}N_3CoO_5PCl$ (354.55): C, 27.10; H, 3.13; N, 11.85 %， Found: C, 26.45; H, 3.35; N, 11.56. IR (KBr, cm^{-1}) 3415 (b), 3137 (w), 2789 (w), 1547 (s), 1334 (m), 1252 (m), 1221 (w), 1136 (m), 1059 (m), 930 (m), 833 (w), 741 (m), 586 (w), 547 (m), 454 (w). Attempt to direct synthesis of **Coptz-2** using $CoCl_2 \cdot 6H_2O$ to replace of $Co(NO_3)_2 \cdot 6H_2O$, and then following the sample procedure of **Coptz-1** was failed.

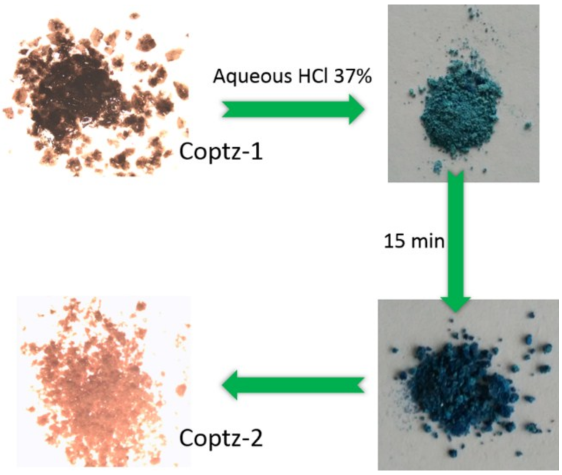

Direct conversion of **Coptz-1** into **Coptz-2** with the presence of LiCl, NaCl, KCl, and HCl in solution was failed.

Direct conversion of **Coptz-2** into **Coptz-1** under H_2O vapor was failed, but it could be realized in hydrothermal treatment condition at 150 °C for 5h.

4. Single-crystal X-ray crystallographic study

Data collection of **Cuptz-1**, **Coptz-1**, **Feptz-1** and **Coptz-2** was respectively carried out on a Bruker Smart CCD diffractometer equipped with graphite monochromated Mo-Kα radiation (λ = 0.71073 Å) at 293 K. Data reduction was performed with SAINT, and empirical absorption corrections were applied by the SADABS program.[2] Structures were solved by direct methods using the SHELXS program and refined with the SHELXL program.[3] Heavy atoms and other non-hydrogen atoms were directly obtained from a difference Fourier map. Final refinements were performed by full-matrix least-squares methods with anisotropic thermal parameters for all non-hydrogen atoms on F^2. C-bonded H atoms were placed geometrically and refined as riding modes. O-bonded H atoms were placed in idealized positions and constrained to ride on their parent atoms. Crystal data as well as details of data collection and refinement are summarized in Table S1. Nos. 906321 (**Coptz-1**), 906323 (**Feptz-1**), 906322 (**Cuptz-1**), 921253(**Coptz-2**) contains the supplementary crystallographic data for this paper. These data can be obtained free of charge from The Cambridge Crystallographic Data Centre via www.ccdc.cam.ac.uk/data_request/cif.

[2]. G.M. Sheldrick, SADABS, Program for Empirical Absorption Correction of Area Detector Data; University of Göttingen: Göttingen, 1996.

[3]. (a) G.M. Sheldrick, SHELXS 97, Program for X-ray Crystal Structure Solution; University of Göttingen: Göttingen.1997; (b) G.M. Sheldrick, SHELXL-97, Program for the Refinement of Crystal Structures, University of Göttingen: Göttingen, 1997.

5. Theoretical fitting of the Magnetic curves

For linear chain, S = 3/2 (**Coptz-1**) and 4/2 (**Feptz-1**), the theoretical expression of susceptibility is presented by Fisher as eq. 1 [4]:

$$\chi_{Chain} = \frac{N\beta^2 g^2 S(S+1)}{3kT} \frac{1+u}{1-u} \qquad \text{(eq. 1)}$$

where $S = 3/2$ and $u = \coth[J \cdot S \cdot (S+1)/(k \cdot T)] - k \cdot T/[J \cdot S \cdot (S+1)]$.

For linear chain, $S = 1/2$ (Cu), we applied the expression as eq. 2 with $x = |J|/k_B T$ [5]:

$$\chi_{chain} = \frac{N\beta^2 g^2}{kT} \frac{0.25 + 0.14995x + 0.30094x^2}{1 + 1.9862x + 0.68854x^2 + 6.0626x^3} \qquad \text{(eq. 2)}$$

For **Coptz-1**, **Cuptz-1**, **Feptz-1**, the interchain interaction (zj', eq. 3) is treated by the molecular field approximation:

$$\chi_m = \frac{\chi_{chain}}{1 - 2zj' / N\beta^2 g^2} \qquad \text{(eq. 3)}$$

All the above symbols have their usual physical meanings and the theoretical fitting to the experimental data was refined by means of a least-squares method. $R = \Sigma[(\chi_M T)_{calc} - (\chi_M T)_{expt}]^2 / \Sigma[(\chi_M T)_{expt}]^2$.

[4]. M.E. Fisher, *Am. J. Phys*. 32 (1964) 343

[5]. J.C. Bonner, M.E. Fisher, *Phys. Rev. A* 135 (1964) 640.

Table S1. Crystallographic data

	Coptz-1	**Copzt-2**	**Cuptz-1**	**Feptz-1**
Formula	$C_8H_8CoN_3O_4P$	$C_8H_{11}ClCoN_3O_5$ P	$C_8H_8CuN_3O_4P$	$C_8H_8FeN_3O_4P$
FW/g mol^{-1}	300.07	354.55	304.68	296.99
Temperature (K)	293(2)	293(2)	293(2)	293(2)
Crystal system	Monoclinic	Monoclinic	Monoclinic	Monoclinic
Space group	P2(1)/c	C2/m	P2(1)/c	*P*2(1)/c
a / Å	10.960(9)	20.71(2)	10.945(5)	11.0479(14)
b / Å	7.193(6)	7.527(8)	7.148(3)	7.2597(9)
c / Å	12.908(11)	8.437(8)	12.967(6)	12.9092(16)
β / °	107.925(9)	99.746(10)	108.675(5)	109.188(2)
V / $Å^3$	968.2(14)	1296(2)	961.1(8)	977.9(2)
Z	4	4	4	4
Dc /g cm^{-3}	2.059	1.817	2.106	2.017
μ/mm^{-1}	1.944	1.672	2.445	1.712
F(000)	604	716	612	600
Total collected	4192	3227	4486	5702
Unique data, R(int)	1896, 0.0639	1288, 0.0276	1725, 0.1074	1736, 0.0244
Completeness	99.6 %	98.7 %	99.8 %	98.7 %
GOF on F^2	1.087	1.050	1.109	1.004
R_1,[a] wR_2[b]$[I > 2\sigma(I)]$	0.0409, 0.1149	0.0353, 0.0949	0.0438, 0.1087	0.0259, 0.0736
R_1,[a] wR_2[b](all data)	0.0431, 0.1163	0.0372, 0.0961	0.0501, 0.1126	0.0320, 0.0979
Peak and hole/e $Å^{-3}$	0.408, -0.859	0.921, -0.599	0.803, -0.527	0.617, -0.555

Table 2. A summary of Coordination parameters, magnetic properties as well as stabilities of **Cuptz-1**, **Coptz-1** and **Feptz-1**.

Sample	Cell	$d_{\text{M-N}}$	$d_{\text{M...M}}$	J cm^{-1}	Coord. Geometry	τ	Stable
Cuptz-1	961.06	2.029(4) / 2.030(4)	3.681	-7.02	square-pyramidal	0.23	rigid
Coptz-1	968.211	2.138(3) / 2.157(4)	3.758	-0.64	square-pyramidal	0.45	Crystal-to-Crystal
Feptz-1	977.855	2.201(3) / 2.189(2)	3.772	-0.28	square-pyramidal	0.34	Collapse

Table S3. The calculated magnetic moments and orbital-projected spin populations inside the atomic spheres of the atoms for **Coptz-1** and **Coptz-2** (the unit is μ_B; the minus sign means the spin down state)

	Site	p_x	p_y	p_z	d_{z^2}	$d_{x^2-y^2}$	d_{xy}	d_{xz}	d_{yz}	Total
Coptz-1	Co	n.a.	n.a.	n.a.	0.6204	0.4276	0.5025	0.4907	0.5097	2.5794
	O1	0.015	0.0032	0.0158	n.a.	n.a.	n.a.	n.a.	n.a.	0.0384
	O2	-0.0128	-0.0089	-0.0188	n.a.	n.a.	n.a.	n.a.	n.a.	-0.0450
	P	-0.0001	0.0000	-0.0022	n.a.	n.a.	n.a.	n.a.	n.a.	-0.0025
	N1	0.0053	0.0026	0.0124	n.a.	n.a.	n.a.	n.a.	n.a.	0.0305
	N2	-0.0131	-0.0052	-0.0023	n.a.	n.a.	n.a.	n.a.	n.a.	-0.0311
Coptz-2	Co	n.a.	n.a.	n.a.	0.2463	0.3713	0.7727	0.6738	0.4783	2.5566
	Cl	0.0377	0.0129	0.0447	n.a.	n.a.	n.a.	n.a.	n.a.	0.1033
	O	0.0104	0.0158	0.0012	n.a.	n.a.	n.a.	n.a.	n.a.	0.0334
	P	0.0008	0.0000	0.0032	n.a.	n.a.	n.a.	n.a.	n.a.	0.0117
	N	0.0108	0.0044	0.0046	n.a.	n.a.	n.a.	n.a.	n.a.	0.0311

Figure S1. (a) Coordination environments of Co(II) in **Coptz-1** (Symmetry code: A: -x, -0.5+y, 0.5-z; B: 1-x, -0.5+y, 0.5-z; (C) -1+x, y, z); (b) the infinite chain in **Coptz-1**, showing the terminal H_2O and the cobridges of phosphonate and triazole groups; (c) 2D layer structure of **Coptz-1**; (d) Packing diagram of **Coptz-1** viewed along the *a*-axis (the hydrogen bonds were shown in yellow dot lines), (**Cuptz-1** and **Feptz-1** are isostructure to **Coptz-1**); (e) the TG curve of **Coptz-1** (in dark-red solid line), **Cuptz-1** (in red dash line), **Feptz-1** (in dark yellow dot line)

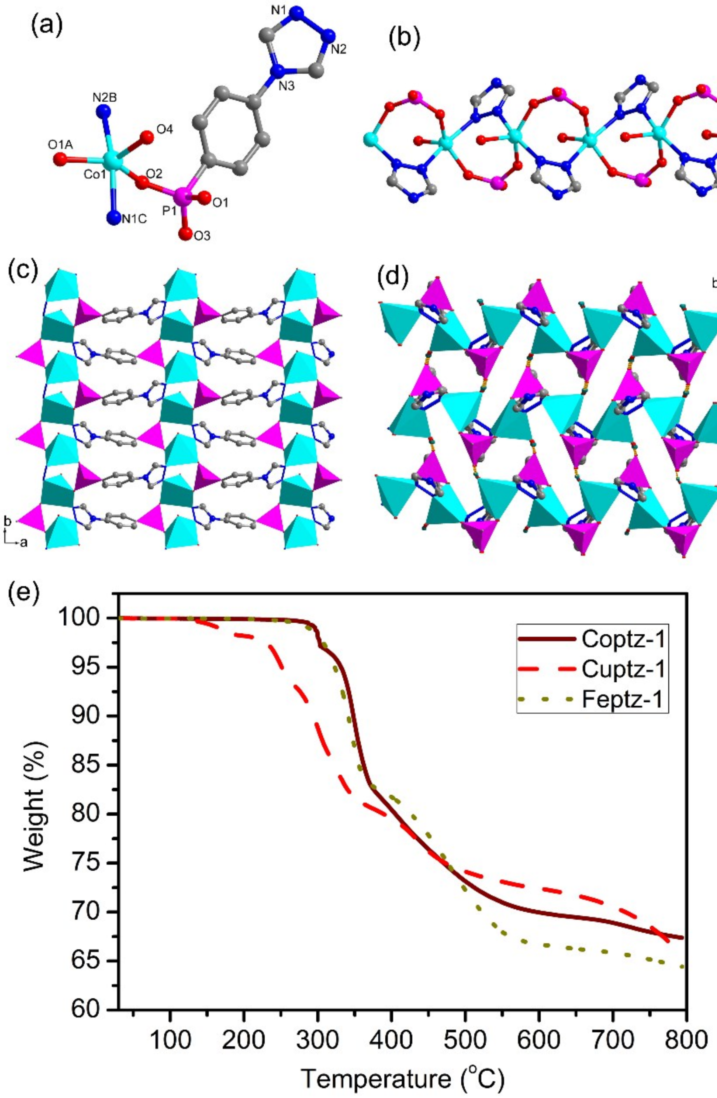

Figure S2. The PXRD pattern shows phase transformation of **Feptz-1** from crystalline solid to amorphous like phase upon HCl vapor (black solid line: simulated from CIF, green solid line: as-made **Feptz-1**; red solid line: HCl chemisorption for 20 min at 30 °C).

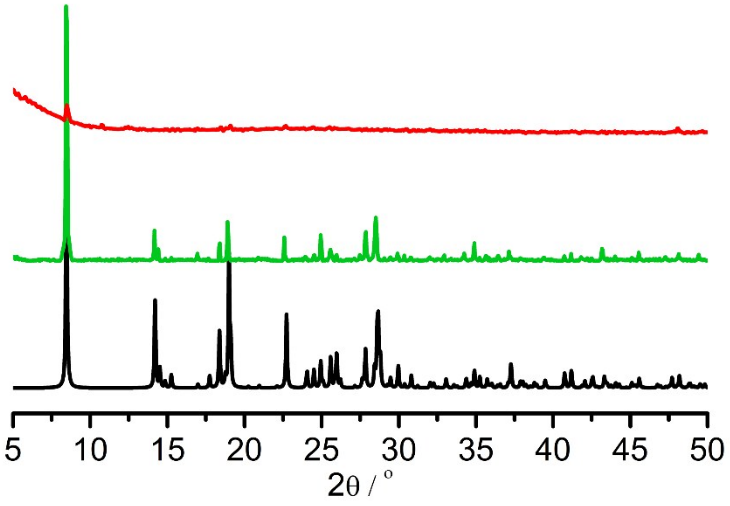

Figure S3. The PXRD pattern shows framework stability of **Cuptz-1** upon HCl vapor (black solid line: simulated from CIF, blue solid line: as-made **Cuptz-1**; dark-yellow solid line: HCl chemisorption for 20 min at 30 °C).

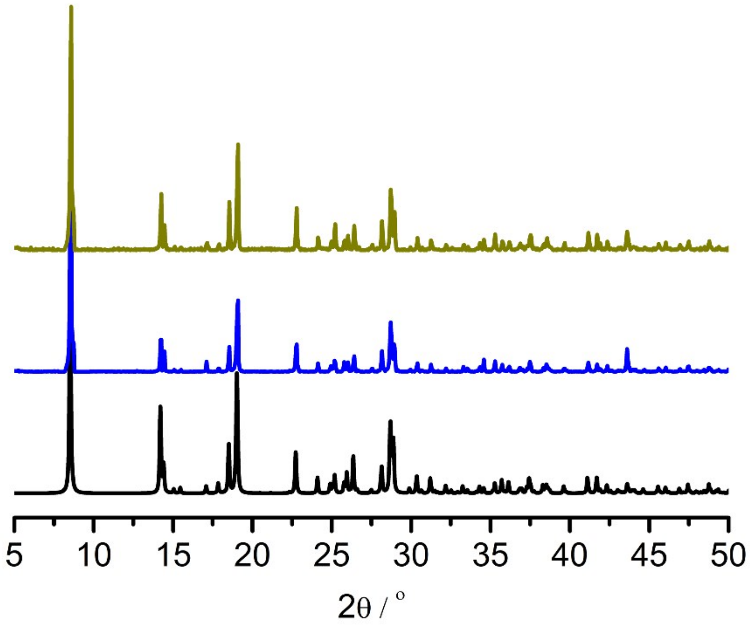

Figure S4. (a) Coordination environments of Co(II) in **Coptz-2** (Symmetry code: A: x, -y, z; B: 1.5-x, 0.5-y, 1-z; (C) 2-x, -y, 1-z; (D) -0.5+x, 0.5+y, z); (b) the infinite chain in **Coptz-2**, showing the μ_2-Cl, phosphonate and triazole groups. (c) 2D layer structure in **Coptz-2**; (d) Packing diagram of **Coptz-2** viewed along the *b*-axis; the hydrogen bonds were shown in yellow dot lines.; (e) the TG curve of **Coptz-2**.

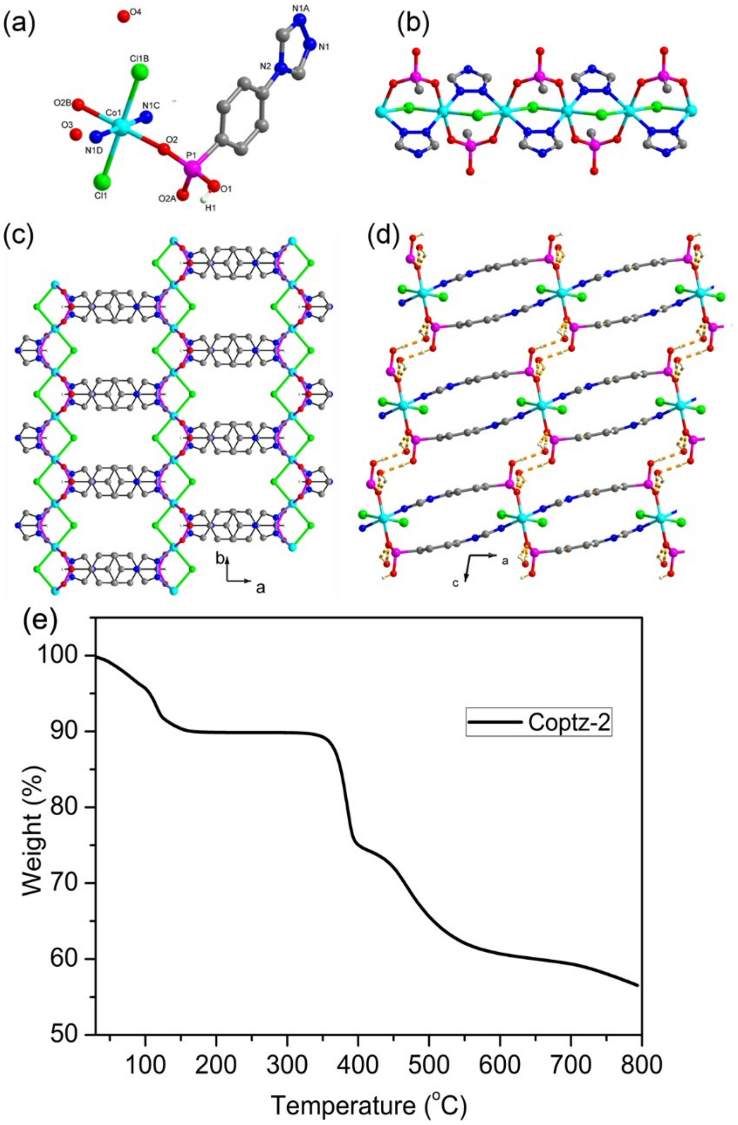

Figure S5. (a) Plots of $\chi_m T$ versus T of **Cuptz-1**, experimental data in open squares with fitted data by eq. 3 in red solid line; (b) Plots of $1/\chi_m$ versus T, experimental data in open triangles with fitted data by Currie-Weiss equation; (c) Plots of magnization versus filed at 2 K, experiemtal data in blue squares and the predicted data by Brillouin function in black dot line ($S = 1/2$, $g = 2.0$)

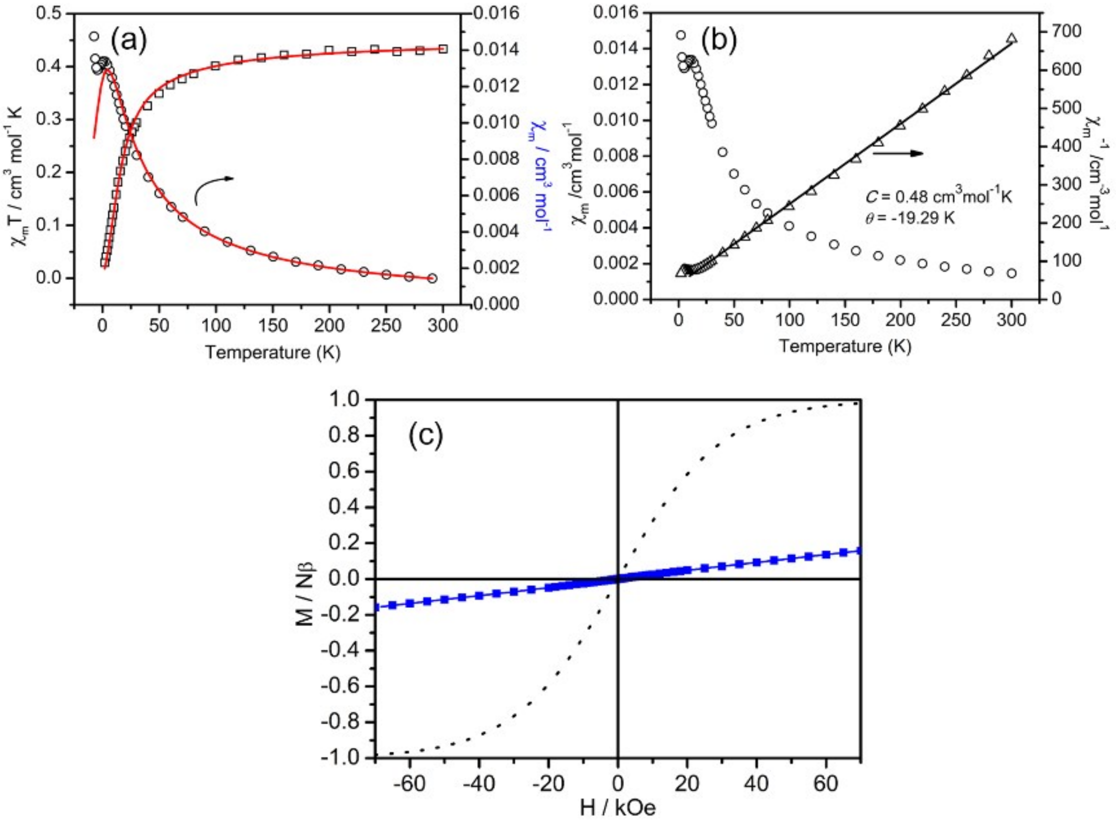

S	1/2
g	2.08(2)
J	-7.02(14)
zJ'	0.06(3)
R	9.94×10^{-4}

Figure S6. (a) Plots of χ_mT versus T of **Feptz-1**, experimental data in open squares with fitted data by Fisher equation in red solid line; (b) Plots of 1/χ_m versus T, experimental data in open triangles with fitted data by Currie-Weiss equation; (c) Plots of magnization versus filed at 2 K, experiemtal data in green squares and the predicted data by Brillouin function (*S* = 2, *g* = 2.0) in black dash line

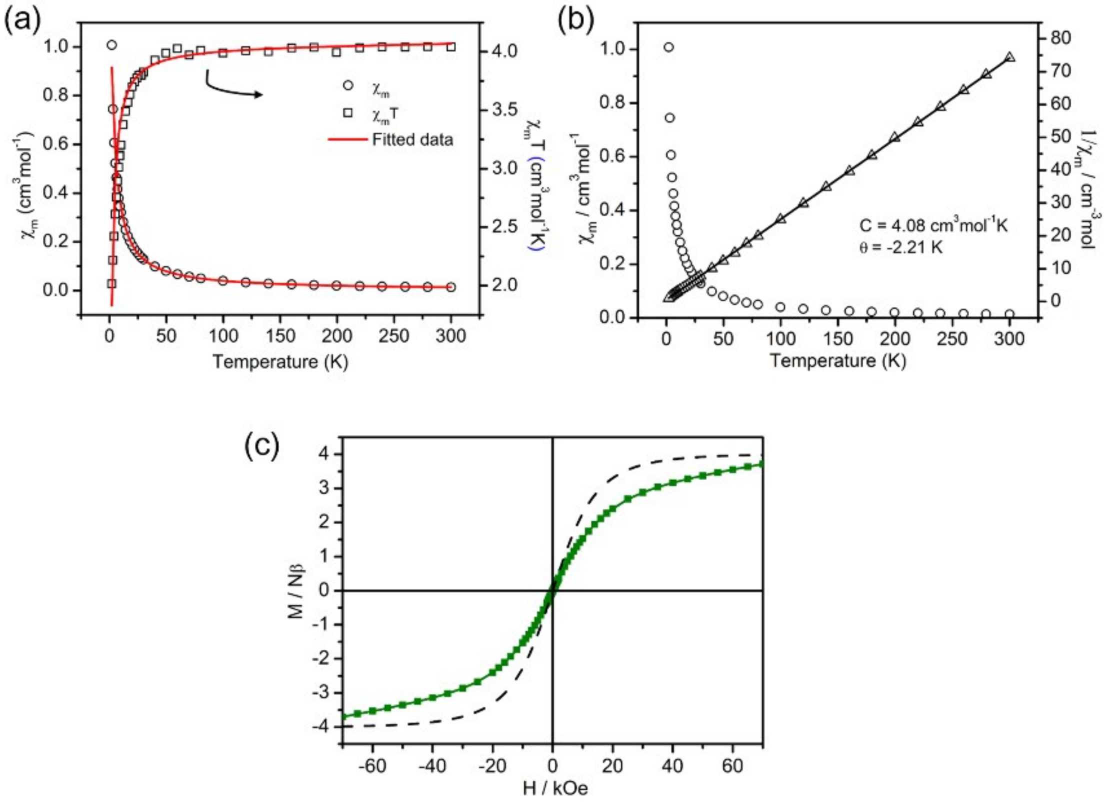

S	4/2
g	2.33(2)
J	-0.29(3)
zJ'	0.32(15)
R	1.55×10^{-3}

Figure S7. (a) The curve of χ_m vs. T (circle) and $1/\chi_m$ vs. T (triangle) for **Coptz-1**, in which $1/\chi_m$ vs. T was fitted by Curie-Weiss function (solid line); (b) The theoretically fitted expeimental data by Fisher equation (eq. 1) with an interchain interaction (*zj*', eq. 3) taking into consideration.

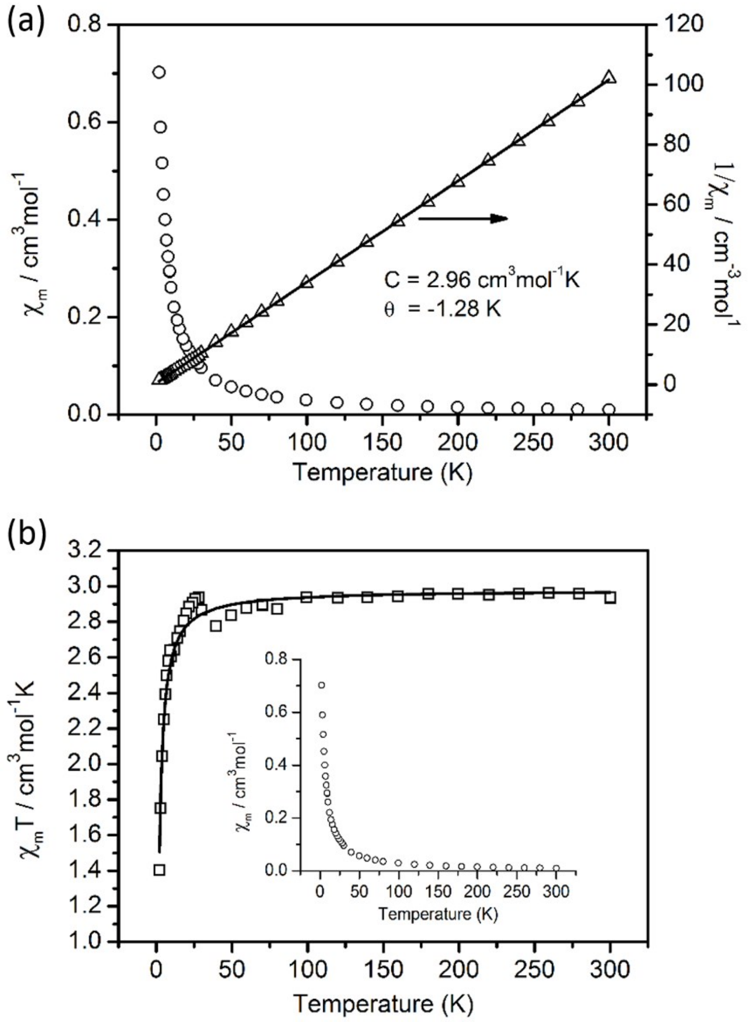

S	3/2
g	2.49(1)
J	-0.64(3)
zJ'	0.83(10)
R	3.27×10^{-4}

Figure S8. (a) The curve of χ_m vs. T (circle) and $1/\chi_m$ vs. T (triangle) for **Coptz-2**, in which $1/\chi_m$ vs. T was fitted by Curie-Weiss function (solid line); (b) Plots of χ_mT versus T. The open squares show raw experimental data and the dotted line stands for spin-orbit coupling effect contributed from $A\cdot\exp(-E_1/k_BT)$ [6]. The subtraction of the raw data from the dotted line results in the blue open squares. The solid line is the fitted result with the Fisher mode [7].

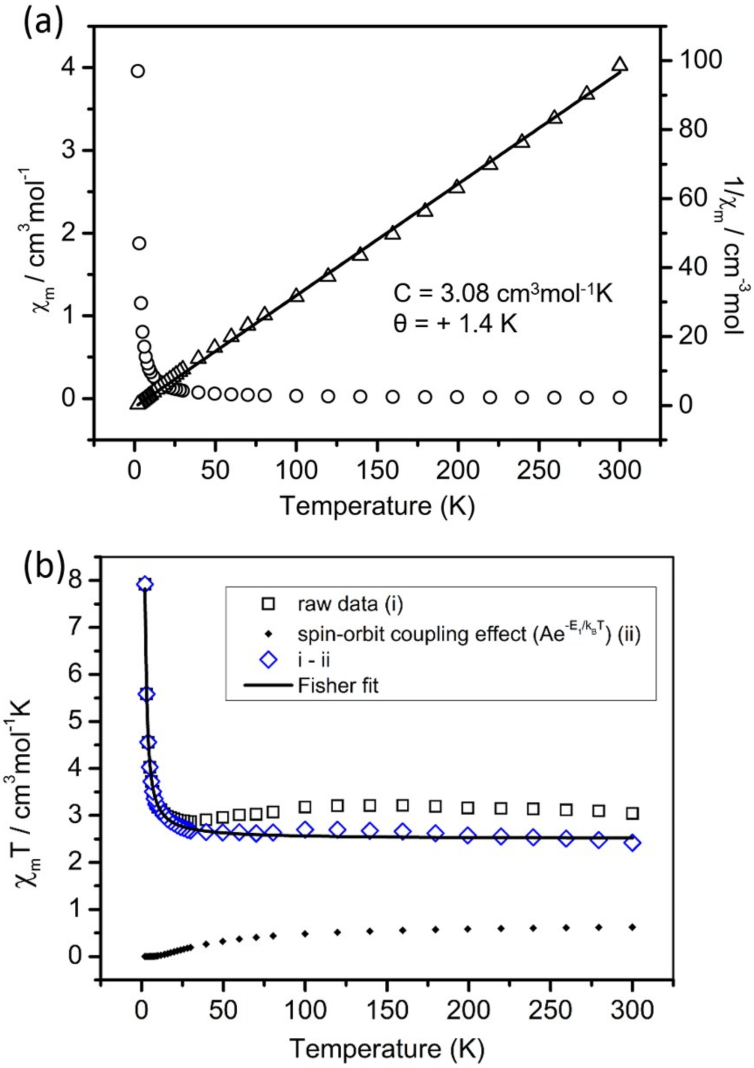

S	3/2
g	2.32(1)
J	0.63(2)
zJ’	0.034(14)
R	2.81×10^{-4}

[6] Rueff, J. M.; Masciocchi, N.; Rabu, P.; Sironi, A.; Skoulios, A., *European Journal of Inorganic Chemistry* **2001**, 2843-2848.

[7] Yoo, H. S.; Kim, J. I.; Yang, N.; Koh, E. K.; Park, J. G.; Hong, C. S., *Inorganic Chemistry* **2007**, 46, 9054-9056.

Figure S9. The partial density of states (PDOS) of 3*d* orbit for Co and 2*p* orbits for O, N, 3p orbits for P and Cl atoms. (a) and (b) for **Coptz-1**, (c) and (d) for **Coptz-2**. The Fermi level (vertical dotted line) is located at 0 eV.

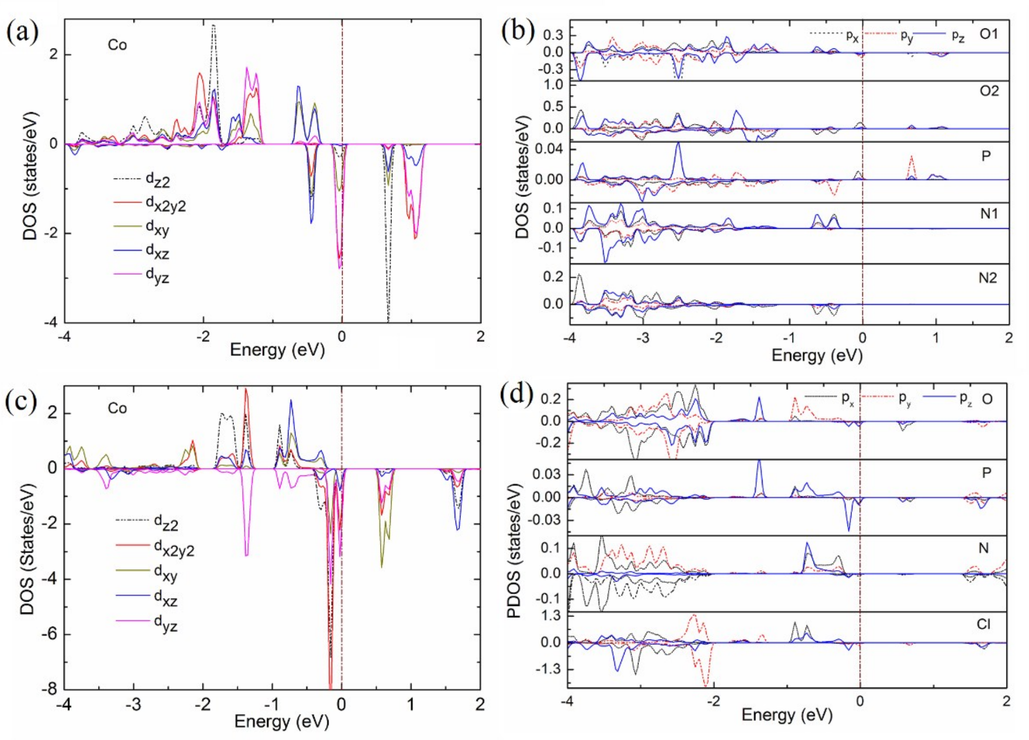

Figure S10. (a) The PXRD patterns confirming the reversible crystal phase transformation from **Coptz-1** to **Coptz-2** by HCl vapor and hydrothermal treatment; (b) a scheme to illustrate the reversible phase trasnformation of **Coptz-1** to **Coptz-2**.